

Flow-level performance comparison of packet scheduling schemes for UMTS EUL

Desislava Dimitrova, Hans van den Berg

Dept. Design and Analysis of Communication Systems
University of Twente
Enschede, The Netherlands

COST 290 TD(07)044

DRAFT

DRAFT

DRAFT

Abstract

UMTS Enhanced Uplink is expected to provide increased data rates and smaller latency on the communication link from users towards the network. In this paper we focus on the performance of various packet scheduling schemes for sharing the EUL shared channel. In particular, we conduct a comparison between three Round Robin scheduling schemes taking into account both the packet level characteristics and the flow level dynamics due to the (random) user behavior. Using a hybrid analytical and simulation approach we analyzed the three schemes with respect to performance parameters such as file transfer time and fairness.

Keywords: UMTS, Enhanced uplink, scheduling,

1. Introduction

As HSDPA for the downlink, EUL uses a shared channel with packet scheduling in order to support enhanced uplink communication, see e.g. [5]. The user access to the channel is organized in timeslots with fixed length, termed TTI (Transmission Time Interval). The short nature of the TTI (2 ms) and fast link adaptation enables higher data transfer rates than 'plain' UMTS.

In contrast to HSDPA for the downlink, due to battery-limited power, a single 'uplink' user cannot use the total available channel resource on its own when it is scheduled. Hence, there is an open opportunity for simultaneous transmissions on the uplink. The several possible scheduling approaches resulted in a diversity of studies, see e.g. [2], [5]-[10]. In our research we set the goal to compare the performance of different scheduling schemes on a UMTS uplink, where we are particularly interested in the influence of flow-level dynamics due to flow (file) transfer initiations by the users at random time instants (i.e. the number of ongoing flow transfers varies over time). We aim to quantify performance parameters such as mean time to transfer a file and fairness.

Roughly spoken two modelling approaches are followed in the literature. Simulation models incorporate all packet level details of the channel operation, but tend to require a lot of time for running the simulation. On the other hand, analytical models, usually primarily aiming at providing insight into the system behaviour at flow level, have to

abstract from packet level details in order to keep them tractable. Both types of models do not satisfy all our requirements and therefore we combined their advantages in a hybrid modelling approach. We use time scale decomposition with small time scale on the packet level analysis (start phase) and bigger time scale on the flow level analysis (main phase). The general nature of the approach allows us to continually expand the research with more detailed system characteristics.

Our modelling and analysis approach consists of three steps. The first two steps mainly deal with the packet level. We start with accounting for the scheduler's behaviour with packet level parameters such as transmission power, distance to the base station and channel interference. Subsequently, we derive in step wise manner an expression for the throughput that an active user obtains in a given state of the system (i.e. the number of active users and their distance to the base station). These throughputs and the rate at which new uplink users become active are used to create a continuous time Markov chain describing the system behaviour at flow level. This is the last modelling step. The Markov model includes the flow dynamics since a state transition actually represents flow initiation or flow completion. From the steady state distribution of the Markov chain the performance parameters, such as mean file transfer time of a user, can be calculated. For some schedulers analytical solution of the steady state distribution can be found, while for others this is not feasible. In the second case fast simulation of the Markov chain is used.

At this point of our research, we compare three possibilities for Round Robin (RR) scheduling. This comparison is the first step towards a research of wide variety of schedulers including channel aware schedulers as well.

The rest of the paper is organized in five sections. Beginning with Section 2, which introduces the schedulers we examine, we move forward to explain our proposed approach in Section 3. There also the assumptions made are stated. Analytical models of the examined schedulers are covered in Section 4. Section 5 presents and discusses numerical results. Finally, in Section 6, conclusions and our plans for future work are given.

2. Scheduling schemes for EUL

One of the basic scheduling schemes is Round Robin (RR) in which all users with non-empty buffers - active users - are served in a cyclic order. A cycle is then the total time necessary to serve all active senders. In a RR scheduler all active senders receive an equal chance to access the channel. The scheduler does not differentiate between active senders with different channel conditions (i.e. channel unaware scheduling). Three different variants of the RR scheduler were investigated, termed one-by-one (OBO), partial parallel (PP) and full parallel (FP). The strategies differ in the number of active senders that are given simultaneous channel access in the same TTI.

A common notion in the three schemes is the available channel resource, termed total interference budget. The total interference budget is the product of the noise rise at the base station and the thermal noise. Part of the total budget is not usable because of interference, for example thermal noise. What is left over we term data budget B' and is the actually available for data transmission channel resource. Since the interference levels in the three schemes differ, the data budget is also changing.

Interference can originate in sources such as base station (thermal noise), own-cell senders (intra-cell interference), other-cell senders (inter-cell interference). In the present study we limit the sources of interference, which is done in Section 3.

One by one scheme

In the first RR strategy – one by one – a single active sender is allowed to use the total channel resource and it can transmit at its maximum power level; see Figure 1, [8]. Although a single transmission is seen as positive because of high achievable rate, it is also a disadvantage. A single active sender can hardly utilize the total channel resource. What part of the resource is unused depends on the sender's channel conditions. Good conditions – close to base station, low interference – result in less unused resource than bad conditions.

Partial parallel scheme

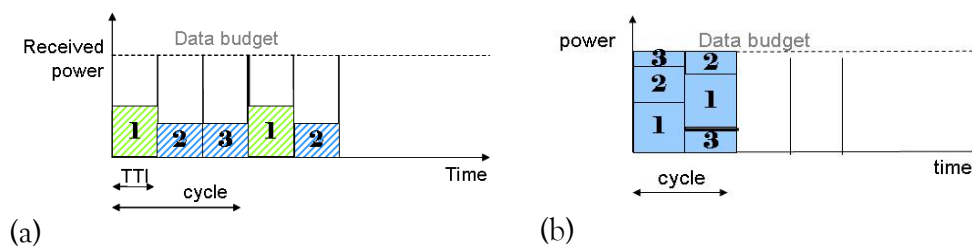
Clearly, the OBO strategy leaves space for optimization. An attempt for full channel utilization is the PP strategy. According to it multiple active senders can simultaneously access the channel in one TTI; see Figure 1. Note that multiple does not mean all active senders. The latter is why we used 'partial' in the name.

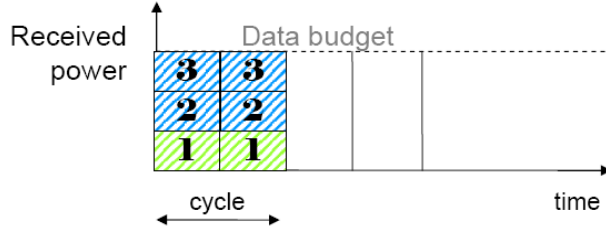
Several ways to organize simultaneous transmissions are possible. We chose a possibility where all selected users use their maximum transmit power and the channel resource is completely used. In the chosen strategy, in the same TTI, users are added until the channel resource is filled up. It is very probable that the last sender will not fit in and its transmission is split in two consecutive TTIs. In this way the total channel resource is utilized. (Of course, there are other possible strategies to deal with filling up the last part of the available budget, but the differences between the possible strategies are expected to be small).

The PP strategy introduces a new source of interference: all active users which are selected to transmit in the same TTI (also termed correlated senders).

Full parallel scheme

The last scheduling scheme of our interest is the full parallel which also allows full utilization of the channel resource. In this scheme all active senders are given simultaneous access in one TTI; see Figure 1, [8]. Consequently each active sender transmits in each TTI until his buffer is empty. When the totally requested resource is more than the channel resource, the transmitting power levels of the active senders are lower than the maximum. The interference sources are the same as for the partial parallel scheme.





(c)

Figure 1 RR scheduling schemes: (a) one by one, (b) partial parallel, (c) full parallel

Some initial observations on the three RR schedulers are possible. For example, the OBO strategy appears to be more advantageous than PP and FP because of the less interference experienced by the senders. On the other hand, the PP and FP strategies show more potential for optimal utilization of the channel resource. Another observation is that FP has the shortest cycle - one TTI - because all active senders are served in one TTI. As a result a single active sender has more frequent access to the channel than in OBO or PP. However, in FP the transmit power is lower, what may be a disadvantage.

With the goal to examine the schedulers in further detail, we developed a modelling approach, which allowed us to look at performance parameters. These parameters give us a more precise, formal way to evaluate the operation of the schedulers. We present the parameters in the subsequent section 3.

3. Modelling assumptions and preliminary analysis

From now on we assume that there are only HSUPA users (using EDCH) and no other ones (e.g. using DCH). Furthermore, during the development of the 3-steps approach we made several assumptions which we summarize here:

- A single cell scenario is researched. The cell is split in K zones with the first zone being the closest to the base station. Each zone is characterized by a distance d_i to the base station and a corresponding signal loss $L(d_i)$; see Figure 2.
- Active users are uniformly distributed in the cell. Their distribution over the zones in the cell is referred to as *state* \underline{n} and has a vector form (n_1, n_2, \dots, n_K) .
- New users become active - have a file to transmit - according to a Poisson process with total rate λ . The probability of arrival in zone i q_i is calculated as the ratio of the area of zone i and the total cell area (implication from uniform distribution). The arrival rate per zone λ_i is then $\lambda * q_i$.
- All active senders have the same maximum transmitted power P_{\max} but different received power at the base station $P_{i, \max}^r$ because of different signal loss.
- The file size has an exponential distribution with mean F (bits).
- Active senders are not mobile (the same position is kept).
- Interference is limited to: (1) assumed as constant thermal noise N ; (2) self-interference; (3) interference from correlated senders I_{corr} .

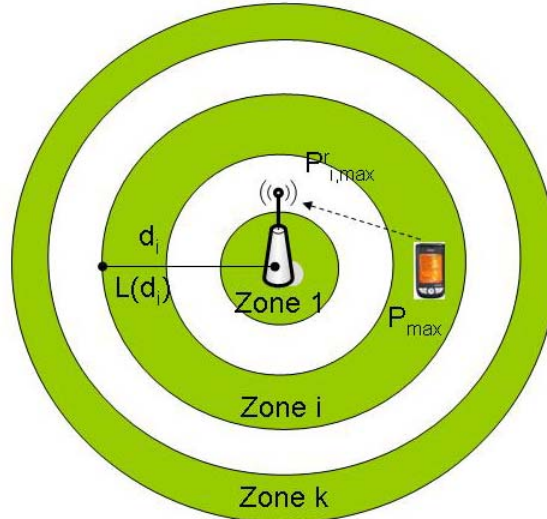


Figure 2 Single cell split in zones

Instantaneous rate

In the packet level analysis – Step 1 and Step 2 – we are dealing with parameters such as: system chip rate R_{chip} , energy per bit to noise ratio E_b/N_o , received power level and interference. In Step 1 we determine what we term instantaneous rate $r_i(\underline{n})$. This is the transmission rate a user in zone i can achieve when it is scheduled, i.e. actually sends data. The instantaneous rate is defined within the boundaries of a TTI and is dependent on the zone, i , in which the user is located, the current state \underline{n} of the system and the scheduling scheme. In general terms $r_i(\underline{n})$ is given by (see [4]):

$$r_i(\underline{n}) = \frac{R_{chip}}{E_b/N_0} * \frac{P_{i,max}^r}{N + I_{corr}(\underline{n}) - \omega P_{i,max}^r}, \quad (1)$$

The received power of an active sender from zone i is marked as $P_{i,max}^r$. $I_{corr}(\underline{n})$ represents the interference from all correlated (i.e. simultaneously scheduled) senders including the own signal. To represent the correct level of self interference, a fraction ω of the own signal is subtracted from $I_{corr}(\underline{n})$. Since $I_{corr}(\underline{n})$ is dependent on the state \underline{n} and the scheduling scheme, such is also the instantaneous rate $r_i(\underline{n})$.

State dependent throughput

Knowledge of $r_i(\underline{n})$ is not sufficient to determine the user's throughput since an active user often has to wait several TTIs between actual data transmissions (scheduling cycle). The result is a decreased effective transmission rate, which we term *state dependent throughput* (SDT) $R_i(\underline{n})$. More precisely, $R_i(\underline{n})$ is the average transmission rate an active user achieves during one cycle, given that the system is/remains in state \underline{n} . Introducing population factor $f_p(\underline{n})$, which is the reciprocal to the cycle length (and dependent on the cell population and the scheduler), we have:

$$R_i(\underline{n}) = r_i(\underline{n}) * f_p(\underline{n}), \quad (2)$$

Flow level Markov model

After the packet level analysis is completed we can introduce flow dynamics. This happens in Step 3 of the analysis with the creation of a continuous time Markov chain model describing the behavior of flow transfer initiation and completions by the users in the cell. The states in the Markov model represents precisely the distribution $\underline{n}=(n_1, n_2, \dots, n_k)$ of the active users over the zones in the cell. State transitions represent initiation of a new flow - jump forward - or completion of an existing flow- jump backward. Hence the Markov model itself is K dimensional with each dimension corresponding to a cell zone. The transmission rates in the Markov model are given by:

$$\begin{aligned} (n_1, n_2, \dots, n_i, \dots, n_k) &\rightarrow (n_1, n_2, \dots, n_{i+1}, \dots, n_k) : \lambda_i = \lambda^* q_i, \\ (n_1, n_2, \dots, n_i, \dots, n_k) &\rightarrow (n_1, n_2, \dots, n_{i-1}, \dots, n_k) : \frac{n_i}{F} * R_i(\underline{n}). \end{aligned} \quad (3)$$

An example for two zones is shown in Figure 3.

From the steady state distribution of the Markov model we can derive the desired performance parameters - the mean file transfer times for the different zones and the fairness.

For the OBO scheduler the steady state probabilities of the Markov model can be derived in closed form from the balance equations. For the PP and FP schedulers the Markov chain has a more complex structure and the steady state distribution cannot be obtained analytically in terms of explicit formulas. We therefore use simulation to determine (estimate) the steady state distribution.

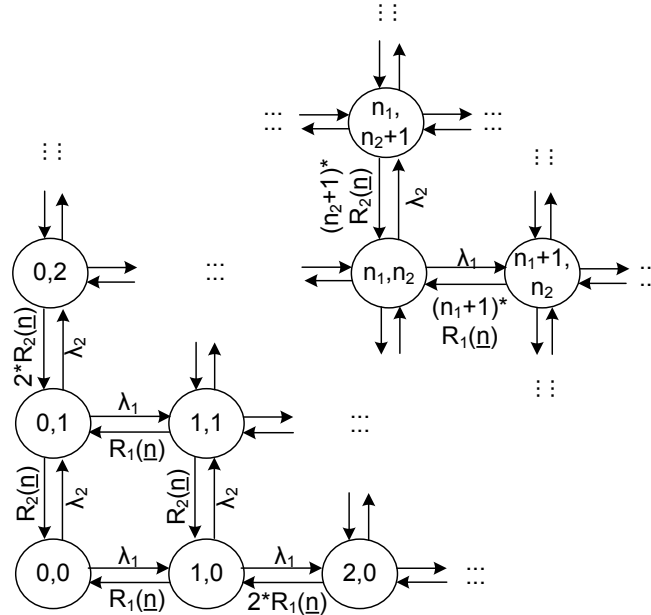


Figure 3 Markov model for two zones

4. Models of the RR schedulers

Following the general 3-steps approach described in the previous section we can analyze various schedulers. As noted before, the difference between the schedulers will be reflected in the different $r_i(\underline{n})$'s and $f_p(\underline{n})$'s resulting into different Markov models describing the flow level behaviour.

4.1. *One By One scheduling scheme*

Sources of interference in the OBO scheduler are thermal noise and the self interference. $I_{corr}(\underline{n})$ in this case consists only of the own signal power, which allows (1) to be re-written as:

$$r_i(\underline{n}) = r_i = \frac{R_{chip}}{E_b/N_0} * \frac{P_{i,max}'}{N + (1-\omega)P_{i,max}'}, \quad (4)$$

Note, that in the OBO scheme the instantaneous rate does not depend on \underline{n} . Moving to Step 2 of the analysis, having only a single active user in a TTI yields a cycle length of $n=n_1+n_2+..+n_K$ (for state \underline{n}). Hence, $f_p(\underline{n})=1/n$ and the state-dependent throughput $R_i(\underline{n})$ is given by:

$$R_i(\underline{n}) = r_i(\underline{n}) * f_c(\underline{n}) = \frac{R_{chip}}{E_b/N_0} * \frac{P_{i,max}'}{N + (1-\omega)P_{i,max}'} * \frac{1}{n}. \quad (5)$$

Expression (4) shows that $R_i(\underline{n})$ depends on the current state \underline{n} only via $f_p(\underline{n}) = 1/n$.

The resulting OBO Markov model, Step 3 of the analysis, is actually a M/M/1 processor sharing model with multiple customer classes. The model is well examined and an explicit expression for the steady state distribution is available, see e.g. [1]:

$$\Pr\{N_1 = n_1 \dots N_k = n_k\} = (1 - \rho) * \frac{(n_1 + \dots + n_k)!}{n_1! \dots n_k!} * \prod_{i=1}^K \rho_i^{n_i}, \quad (6)$$

where ρ is defined as $\rho = \sum_{i=1}^K \rho_i$ and $\rho_i = \lambda_i / r_i(\underline{n})$.

From the steady state distribution, using Little's formula [3], the mean time \hat{T}_i to transfer a file for a user in zone i can be calculated:

$$\hat{T}_i = \frac{1}{r_i * F} * \frac{1}{1 - \rho}. \quad (7)$$

4.2. *Partial Parallel scheduling scheme*

The PP strategy allows parallel transmissions in one TTI, therefore $I_{corr}(\underline{n})$ is the interference caused by *all* scheduled senders in the TTI. Consequently, the instantaneous rate is dependent on \underline{n} , see (1). This dependency results in a complex expression for the state dependent throughput and eventually creates difficulties for analytical solution. Another factor that turns the PP strategy in a suitable candidate for simulation is the form of $f_p(\underline{n})$.

The opportunity for simultaneous transmissions results in shorter cycle than in one-by-one scheme. The cycle length can be expressed as the ratio of the total requested (by all active senders) resource and the limited channel resource B' . The population factor, as reciprocal to the cycle length, is then given by:

$$f_p(\underline{n}) = \frac{B'}{\sum_i P_{i,max}' * n_i}. \quad (8)$$

Hence the state dependent throughput $R_i(\underline{n})$ depends in several intricate ways on \underline{n} ,

via $f_p(\underline{n})$ and $I_{corr}(\underline{n})$:

$$R_i(\underline{n}) = \frac{R_{chip}}{E_b/N_0} * \frac{P_{i,max}^r}{N + I_{corr} - \omega P_{i,max}^r} * \frac{B'}{\sum_i P_{i,max}^r * n_i}, \quad (9)$$

where $I_{corr}(\underline{n}) = B'$.

Note, that in the special case that the sum of the power levels of the active senders is lower than the budget B' , i.e. $\sum_i P_{i,max}^r * n_i < B'$, each active user sends in each TTI

and the population factor is $f_p(\underline{n}) = 1$. That affects the calculation of the state dependent throughput:

$$R_i(\underline{n}) = \frac{R_{chip}}{E_b/N_0} * \frac{P_{i,max}^r}{N + I_{corr} - \omega P_{i,max}^r}, \quad (10)$$

where $I_{corr}(\underline{n}) = \sum_i P_{i,max}^r * n_i$.

Consequently the resulting flow level Markov model is a complex processor sharing type of queuing model with transition rates that depend on the detailed state distribution $(n_1, n_2 \dots n_K)$. Due to this we chose to simulate the flow level Markov model of the PP scheduler in order to determine the steady state probabilities.

4.3. Full Parallel scheduling scheme

An active user in the full parallel scheme transmits in each TTI and therefore the population factor $f_p(\underline{n})=1$ for all states \underline{n} . That means that the state dependent throughput is equal to the instantaneous rate, i.e. $R_i(\underline{n})=r_i(\underline{n})$. $I_{corr}(\underline{n})$ in $r_i(\underline{n})$, see (1), is caused by all active users. We distinguish between two cases. In the first case the number of active users is such that the sum of their (received) maximum powers is lower than the data budget B' . Then the senders use their maximum transmit power and the state dependent throughput is the same as in PP, see (10). The second case is when the summed maximum received power from all senders is higher than the data budget. Since all senders transmit in parallel, the transmission power levels have to be decreased such that the summed received powers fit in the data budget. The resulting received power levels P_i^r are derived from the maximum received power via proportional decrease,

$$P_i^r = \frac{P_{i,max}^r}{\sum_{i=1}^k P_{i,max}^r * n_i} * B', \quad (11)$$

such that $I_{corr}(\underline{n}) = \sum_i P_i^r * n_i = B'$.

Using P_i^r we can rewrite (1) for this second case of FP as:

$$R_i(\underline{n}) = r_i(\underline{n}) = \frac{R_{chip}}{E_b/N_0} * \frac{P_i^r}{N + B' - \omega P_i^r}. \quad (12)$$

Since $R_i(\underline{n})$ depends on the full state information $(n_1, n_2 \dots n_K)$ the resulting flow level Markov model for the FP scheme showed to be – similar to the PP scheme – a complex processor sharing type of queuing model. Again simulation of the Markov model was used to derive the steady state distribution from which the performance measures were derived.

5. Numerical results

The comparison of the three scheduling schemes is based on performance parameters such as mean file transfer time for zone i , mean number of active users in zone i , and

fairness. The fairness is defined as the ratio of the mean file transfer times in zone K and zone 1. In our numerical example the cell is split in 10 zones, i.e. $K=10$, see Figure 2. As zone radius is taken the distance from the outer boundary of the zone to the base station. Given a certain E_b/N_o , maximum transmission power and worst case interference (all data budget is used), we determined the zone radius such that instantaneous rates starting from 256 kbps for zone 10 up to 4096 kbps for zone 1 are achievable. The performance parameters are generated for a range of increasing arrival rates.

Physical and link layer parameters

The system chip rate R_{chip} is a fixed parameter of 3840 kchips/s. We set for all zones independently from the achievable rate - the same E_b/N_o target of 1.94. The thermal noise N and the noise rise NR at the base station are -135.66 dB and -6 dB, respectively. From these two parameters the data budget (-130.9 dB) can be calculated by $B^2=NR*N*N$ (Watt). The maximum transmission power P_{max} for all users is set to 0.125 Watt. Finally, self interference of half the own signal is considered, i.e. $\omega = 0.5$. All chosen values are based on observations of existing networks.

Simulation of flow level Markov chain

Since the OBO scheduling scheme yields an analytically solvable flow level Markov model we can use explicit formulas to generate the performance parameters. For the PP and FP schemes we simulated the flow level Markov chain, in order to obtain its steady state distribution, and next we determined the system performance parameters. We created a generic simulator for multi-dimensional Markov chains by using MatLab [MatLab]. Note, that we actually just simulate state transitions taking in account the transition rates from the flow level Markov model, cf. [11]. In particular, given the currently visited state \underline{n} , we calculate the total rate out of the state, denoted by $Q(\underline{n})$, as:

$$Q(\underline{n}) = \sum_i \lambda_i + \sum_i R_i(\underline{n}).$$

Subsequently, the transition probabilities are calculated as:

$$\Pr\{\text{forward jump in dimension } i\} = \lambda_i/Q(\underline{n}), \quad i = 1, \dots, K,$$

$$\Pr\{\text{backward jump in dimension } i\} = R_i(\underline{n})/Q(\underline{n}), \quad i = 1, \dots, K,$$

and a uniform sample is used to determine which transition takes place. Before moving to the newly chosen state the time spent in the current state is taken as a sample from an exponential distribution with mean $1/Q(\underline{n})$.

By applying this iterative process for 1 million jumps and collecting data on the total time spent in each visited state, we derived the steady state distribution. Note, that just simulating the jumps in the Markov chain requires relatively short running times. For example, our simulations (one million jumps) took typically 2-2.5 minutes (and can be speed up considerably). This eases multiple simulation runs and statistics such as confidence interval.

As we mentioned the numerical results were generated for increasing arrival rates. The range was taken such that the system load with OBO scheme varies from 0 to the value where the system becomes saturated. Note that this value depends on the scheduling scheme and self-interference. The presentation and discussion of the results is split in four major items, see below.

System saturation

We observed from simulation that the OBO scheme reaches saturation for a lower arrival rate than the PP and FP schemes. That can be seen in Figure 4. (in particular graph a). In particular, for $\lambda=1.6$ the system with OBO scheduling is unstable (in fact $\rho>1$ in formula (6)). These results illustrate the essential drawback of OBO, i.e. this scheme is not able to completely exploit the available resources.

Mean file transfer time

The graphs a-c in Figure 4 show the mean file transfer time for the three scheduling schemes. Additionally in a separate graph (d) combined results for the three schemes are shown in order to ease their comparison. Note that the scale on the y-axis of the figures is not the same.

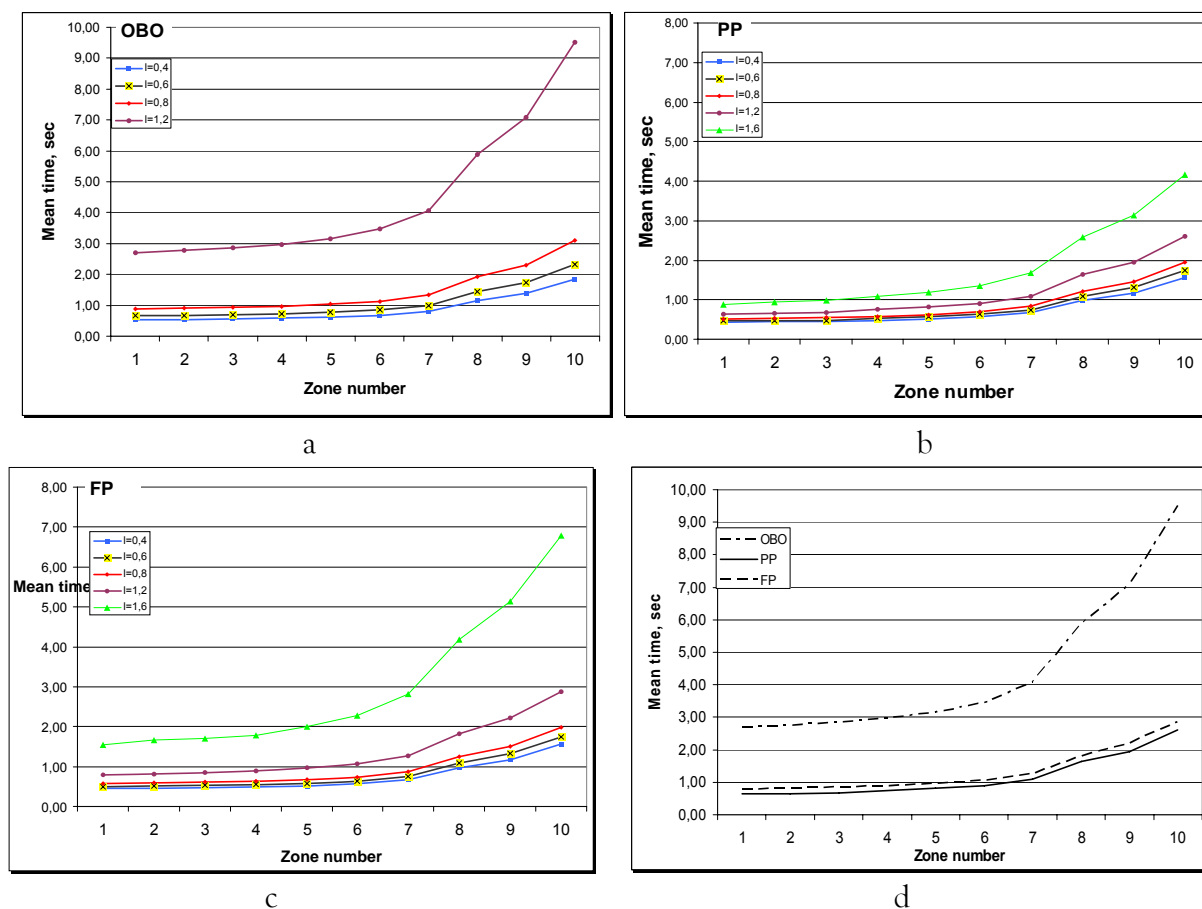


Figure 4 Mean file transfer time for RR schemes: a – one-by-one scheduler, b – partial parallel, c – full parallel, d – combined graph, $\lambda=1.2$

For each of the three schemes we observe, as expected:

Result1: Increase in the arrival rates, respectively the load, leads to longer mean file transfer time.

Cause1: The system is busier and a sender comes less frequently on the turn, therefore longer time is necessary to transfer the same file.

Result2: Further away zones need more time for file transfer than closer zone.

Cause2: Further away zones have lower instantaneous rates therefore they need more time for transfer.

Result3: With a very high arrival rate (load) the graph slope rapidly increase.

Cause3: The system is more sensitive to load changes when it is close to saturation because of the scarce left over system resource.

Result 4: For low load PP and FP generate the same transfer times while for high loads PP shows lower transfer times than FP.

Cause 4: Recall that the state dependent throughputs for PP and FP are the same if the number of active users is low, see formula (10), which is typically the case when the load is low. With increased number of active users (i.e. higher loads) the state dependent throughputs for PP and FP become different, see (9) and (12), and therefore also the results on the mean transfer time differ.

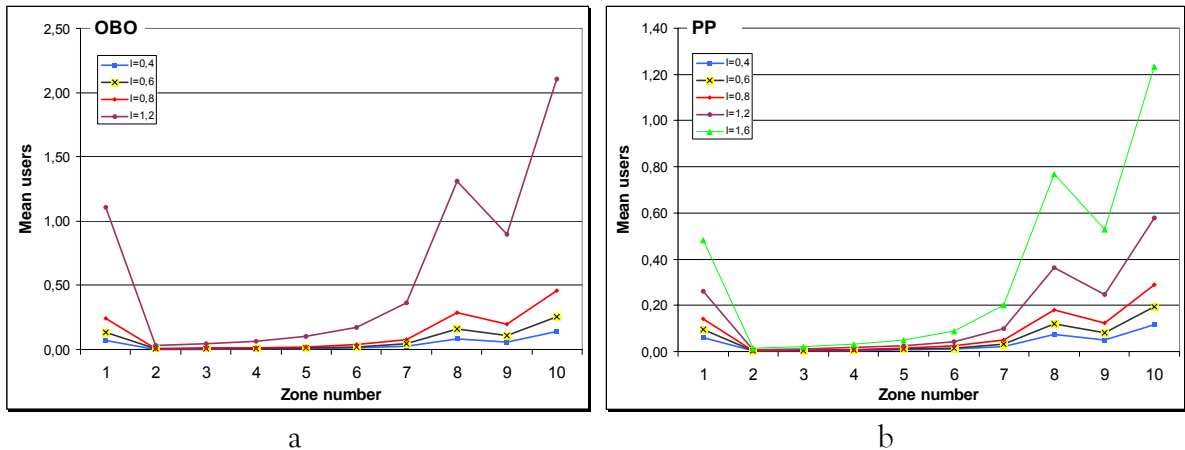
Result5: PP has the smallest mean file transfer time.

Cause5: PP vs. OBO: more frequent transmissions (in PP) lead to increase in the state dependent throughput $R_i(\underline{n})$, which compensates for the larger $I_{corr}(\underline{n})$. PP vs. FP: maximum transmission power (PP) is more advantageous than increased transmission frequency (FP). To clarify the latter recall expression (1) – higher received power means lower total interference – from $I_{corr}(\underline{n}) - \omega * P_{i,max}^r$ – and therefore higher instantaneous rate.

However, we consider it important to note that the graph of the FP scheme does not lay much higher than the graph of PP. This implies that the effect of decreased transmit power is not as negative as we might have thought in the beginning of this study.

Mean number of active users

We will consider now the results in terms of the mean number of active users in each zone, see Figure 5. Again some observations were done.



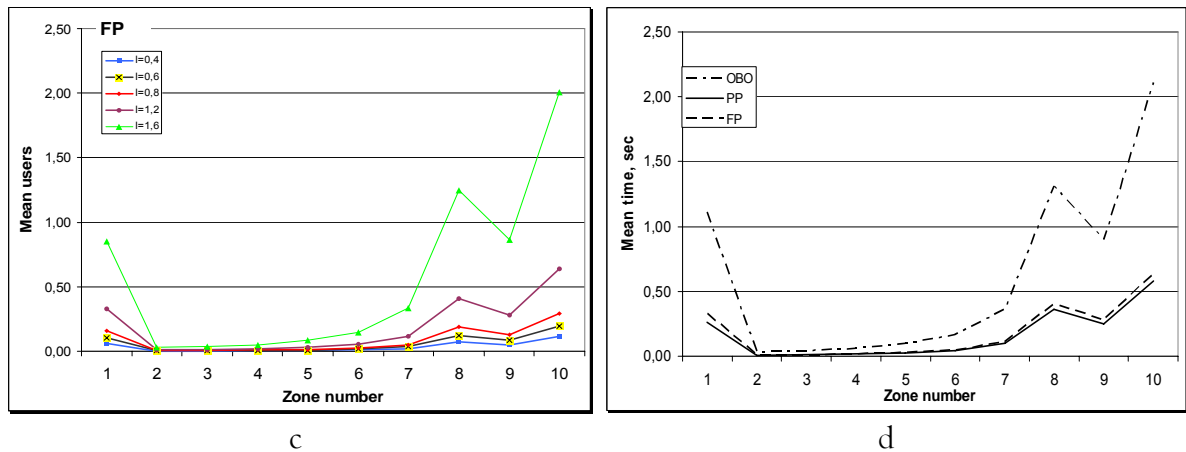


Figure 5 Mean number of active users for RR schemes: a – one-by-one scheduler, b – partial parallel, c – full parallel, d – combined graph.

Result1: The curves have a varying, ‘turbulent’ shape.

Cause1: Since the difference in zone area is irregular such is also the difference in arrival rates and eventually the mean number of senders; see (6). The low sections – zones 2 to 6 – correspond to low zone arrival rate and the high sections – zone 1 and zones 7 to 10 – to high arrival rate.

As expected, when comparing the three scheduling schemes the PP scheme performs the best, which can be explained again by following the reasoning for the mean file transfer time.

Fairness

Finally, we evaluated the fairness of each scheduling scheme – OBO, PP and FP. The results for different arrival rates are organized in Table 1. The general impression is that there is not much difference between the schedulers.

Table 1 Fairness for RR schemes

	$l = 0,4$	$l = 0,6$	$l = 0,8$	$l = 1,2$	$l = 1,6$
OBO	3,51	3,51	3,51	3,51	-
PP	3,597	3,722	3,77	4,079	4,707
FP	3,492	3,496	3,496	3,592	4,36

<<< Further investigation needed, e.g. role of self-interference factor here >>>

Influence of the self-interference factor ω

The self interference is in fact not a factor we can influence but it is nevertheless a factor which changes with the environment. Therefore we examined scenarios where ω was varied. We observed that the PP and FP schemes are less affected by the change in the self interference than the OBO scheme. Figure 6 presents – for each of the schedulers – the increase in file transfer times corresponding to an increase of ω . We have presented results for $\omega = 0, 0.25, 0.5, 0.75$ and 1. The difference in transfer time for two different values of ω illustrates the influence of the self-interference on the scheduling scheme. Smaller difference in transfer time – less space between the graphs – means that the scheme is

more robust to changes in the self-interference. Figure 6 shows that OBO is the scheme most sensitive to self-interference. Recalling expression (1) can provide an explanation. The elements of interference in OBO – thermal noise and self interference – are of the same numerical scale, while in FP and PP there is an additional interference element $I_{corr}(n)$ of bigger scale. Consequently, increase in ω affects the total interference, the instantaneous rate respectively, in OBO more than in the other two schemes. As a result the difference in file transfer time is bigger.

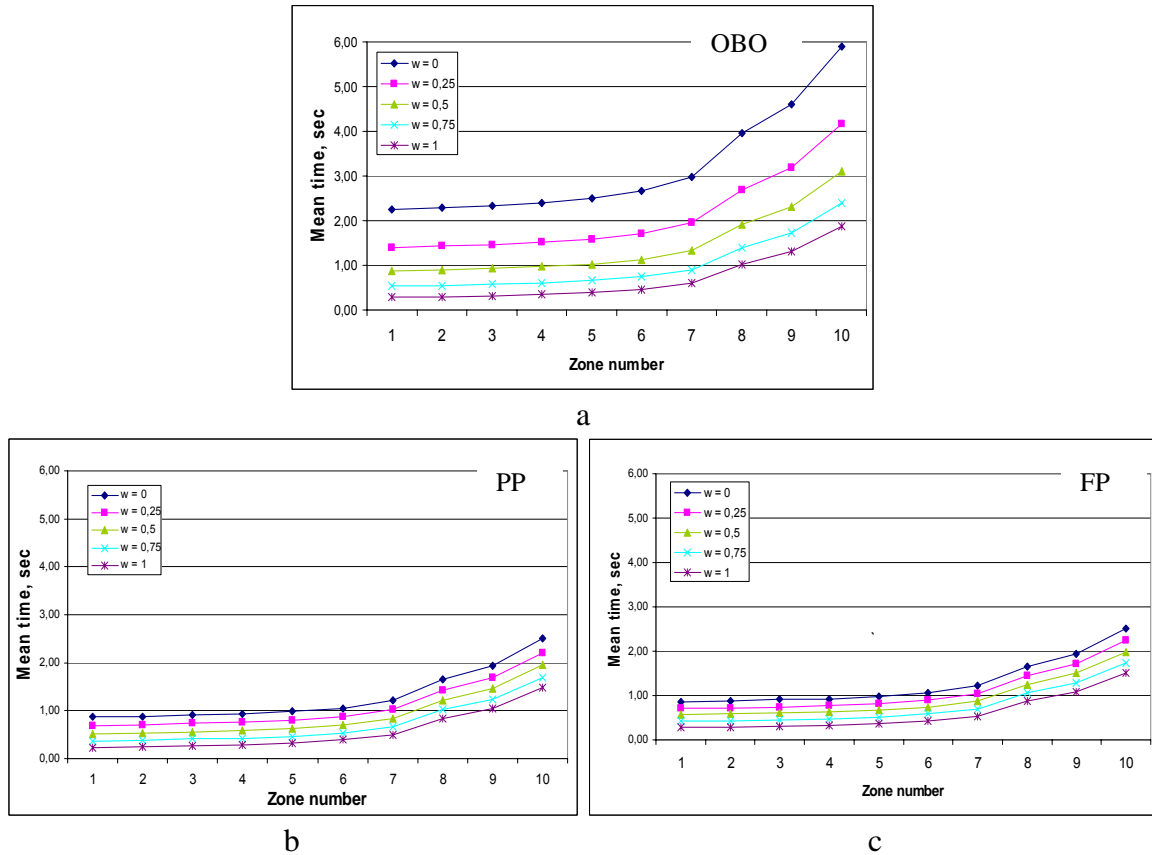


Figure 6 Influence of the self-interference: a – one-by-one scheduler, b – partial parallel, c – full parallel

6. Conclusions

We presented a three-step modelling and analysis approach for comparing the flow-level performance of three Round Robin scheduling schemes for UMTS EUL – One By One (OBO), Partial Parallel (PP) and Full Parallel (FP) scheduling. In the first two steps of our approach the system behaviour at packet level is captured; next, in the third step, based on the packet level behaviour, a Markov chain is created which describes the system behaviour at flow level. From the steady state distribution of the Markov chain (which can be obtained in closed form or numerically, depending on the scheduling scheme), the flow level performance characteristics can be determined.

The considered scenario consists of a single cell divided into zones, and takes into account interference factors such as thermal noise, self-interference and interference from parallel transmissions in the same TTI. The main performance measures in our study were the mean

flow transmission time for the users in each of the zones of the cell and the fairness (i.e. the ratio of the mean flow transfer times for the zone nearest to the base station and the zone at largest distance from the base station). The results show that the PP strategy has the lowest mean file transfer time. This can be explained by the fact that PP has higher transmission power than FP and more frequent transmissions than OBO (i.e. PP exploits the available radio resources most efficiently). Additionally, we showed that the three schedulers do not differ that much in fairness although the FP scheme seems to be slightly outperforming the other two schemes.

We believe that our three-step modelling approach can be extended in order to incorporate more system characteristics in the analysis, see below.

The present study takes in account neither intra-cell nor inter-cell interference. These are however important characteristics of a real network and their influence should be therefore also researched. Currently, we are including the impact of intra-cell interference due to non-EUL (uplink DCH) users in our study. As a second extension we plan to analyse the examined scheduling schemes in circumstances of inter-cell interference.

Finally, instead of the channel oblivious Round Robin schedulers, we will also consider channel aware schedulers, in order to investigate their potential for throughput enhancement and impact on e.g. fairness.

Acknowledgement

The authors would like to thank Geert Heijenk and Remco Litjens for their valuable input and comments.

References

Web sources

[3GPP] <http://www.3gpp.org/specs/releases.htm> (accessed on 17-08-2007)

[Vodafone1]

http://www.vodafone.nl/over_vodafone/pers/persberichten/2004/; Press release N13 (accessed on 17-08-2007)

[Vodafone2]

http://www.vodafone.com/start/media_relations/news/group_press_releases/2006/press_release16_10.html (accessed on 16-08-2007)

[MatLab] <http://www.mathworks.com/> (accessed on 16-08-2007)

Printed sources

[1] H. van den Berg, R. Litjens and J. Laverman, "HSDPA flow level performance", MSWiM'04, 2004

[2] E. C. Haddad, P. Mermelstein and C. Despins, "A transmit assignment algorithm for uplink flow control in WCDMA networks", VTC '99

[3] B. Haverkort, "Performance of computer communication systems", John Wiley & Sons LTD, 1999

[4] H. Holma and A. Toskala, "WCDMA for UMTS", John Wiley & Sons, LTD, 2001

[5] H. Holma and A. Toskala, "HSDPA/HSUPA for UMTS", John Wiley & Sons LTD, 2006

- [6] K. Kumaran and L. Qian, "Uplink scheduling in CDMA packet-data systems", IEEE INFOCOM 2003
- [7] E. G. Lundin, F. Gunarsson and F. Gustafsson, "Robust uplink resource allocation in CDMA cellular radio systems", Proceedings of the 44th IEEE conference on Decision and Control, and the European Control Conference, 2005
- [8] A. Mader and D. Staehle, "An analytical model for best-effort traffic over the UMTS Enhanced uplink", Vehicular Technology Conference, 2006.
- [9] A. Mader and D. Staehle, "Feasible load regions for different RRM strategies for the Enhanced Uplink in UMTS Networks", EuroNGI Workshop, 4396: 213-228, 2006
- [10] S. Ramakrishna and J. M. Holtzman, "A scheme or throughput in a dual-class CDMA system", IEEE J. Select. Areas Commun., vol. 16, pp. 830-844, 1998
- [11] D. Abendroth, H. van den Berg and M. Mandjes, "A versatile model for TCP bandwidth sharing in networks with heterogeneous users", AEU : International journal of electronics and communications, 60 (4). pp. 267-278. ISSN 1434-8411